Copenhagen '12

F038

Towards Joint Interpretation of CSEM Surveys with 4D Seismic for Reservoir Monitoring

O. Salako* (Heriot-Watt University), C. MacBeth (Heriot-Watt University) & L. MacGregor (RSI)

SUMMARY

Here, we generate CSEM data from the fluid flow simulator by performing 1D forward modelling. For this purpose we utilise a heterogeneous model where resistivity is been measured using an inline acquisition geometry. It is observed, that timelapse CSEM surveys can be used to monitor realistic water flood fronts. Changes in the amplitude of the horizontal component, and phase of the vertical component, correlate with water saturation change. The sensitivities of the timelapse CSEM and the 4D seismic to water saturation change in a three phase system with pressure variation are compared using cross-plots. The CSEM is more responsive and consistently more linearly related to water saturation change than the seismic. However, direct measurements of saturation change from CSEM surveys still need to be constrained by knowledge of the spatial distribution of porosity, net-to-gross and reservoir thickness.

Introduction

Time-lapse seismic data are now a well known geophysical tool in reservoir monitoring. However, just like other geophysical methods, the method possesses inherent ambiguities. In particular, separation of pressure and saturation changes can sometimes be difficult with 4D seismic alone (Landrø, 2001; MacBeth et al., 2006). Integration of another geophysical method, which is independently sensitive to only one dynamic reservoir property, could therefore be advantageous to reduce this ambiguity. One such method is marine controlled-source electromagnetic (CSEM) surveying, because of its sensitivity to change in resistivity, which in turn is due to a change in water saturation induced by the reservoir production and injection activities.

Recent sensitivity studies to examine the feasibility of applying CSEM for monitoring have utilised forward modelling of electromagnetic (EM) responses to different reservoir production scenarios. For example, Lien and Mannseth (2008) modelled the timelapse effect of a lateral flooding process using 3D modelling with an integral equation approach. Orange et al. (2009) examined different cases of water flooding and sweep efficiencies, and their corresponding timelapse EM responses using a 2D finite element approach. These two examples showed that production activities could indeed translate to a measurable timelapse CSEM signal and it is possible to interpret the water-flooding front from these signatures. However, the studies assumed a sharp front which is unrealistic in practice. More recently, Shahin et al. (2010) and Liang et al. (2011) utilised a fluid-flow reservoir simulator to take into consideration a realistic vertical profile. Using a 2.5D CSEM approach and 3D finite-difference algorithm respectively, they both confirmed the usability of marine CSEM for reservoir monitoring.

Here, we have taken these studies a step further by incorporating the process for forward modelling of timelapse electromagnetic responses into a flow simulation to seismic workflow. We have done this in order to compare not only the sensitivity but also the correlation to the change in saturation. We determine the best combination of reservoir variables to which the timelapse CSEM is most linearly related. For this, we embed a 3D model of a hydrocarbon producing reservoir within a background resistivity structure. The 1D responses of vertical columns through this model are generated and contoured at the surface to produce the subsequent EM anomaly map.

Simulator to Resistivity (*sim2resist*) modelling

Our modelling is based on the assumption of in-line CSEM acquisition geometry, which has the most sensitivity to reservoir structures. In this geometry, the resulting signals are preferentially sensitive to the vertical resistivity within the reservoir. The vertical resistivity of the reservoir is calculated from the simulator. The reservoir under consideration is a heterogeneous deep-water turbidite system on the UK continental shelf containing sand channels interbedded with shale layers. Thus we assumed a series arrangement of sand and shale resistivities, scaled with the spatial distribution of net-to-gross (NTG). We relate the formation resistivity, R_t, to the petrophysical properties in a simulator cell by modifying Archie's equation (Archie, 1942);

$$R_t = NTG\,\frac{aR_w}{\Phi^m S_w^n} + (1 - NTG\,)R_{sh}\ , \qquad (1)$$

Archie parameters $a = 1$ and $n = 2$ are chosen, while m, the cementation factor and R_w, the formation water resistivity are calculated from well logs. R_{sh}, the resistivity of brine saturated shale is obtained directly from the resistivity log. NTG, Φ *and* S_w, are net-to-gross, effective porosity and water saturation respectively, and their spatially varying distributions are available from the simulator. We assumed that only water saturation is dynamically changing with production activities.

Resistivity to Electromagnetic (*resist2EM*) modelling

The offshore hydrocarbon reservoir is buried at 1.8 to 2.0km below the seafloor with water depth of about 400m. The resistivities of the seawater and the seabed outside the reservoir are 0.3Ωm and 1Ωm respectively, and these values are assumed to be constant with time. The transmitter dipole is towed 25m above the seafloor and parallel to the receiver dipole fixed on the seafloor. The transmitter – receiver spacing increases by 500m from zero up to 15km total offset. Sixteen transmitting

frequencies at equal logarithmic interval between 0.01 to 10Hz inclusive are used. We modified the 1D dipole code of Key (2009) to numerically model EM responses for the CSEM surveys. The reservoir production and injection activities are simulated for 1998 to 2008 inclusive, covering the baseline and ten monitor surveys. As a reconnaissance measure to determine suitable acquisition parameters, we examined the timelapse CSEM responses to the changing resistivity profiles (top row of Figure 1) through a chosen simulator cell after one year, five years and ten years of production and injection activities. This was accomplished by subtracting the baseline response from the monitor response normalised by the baseline response. The percentage changes in the horizontal amplitudes are plotted against the offsets and frequencies for each of the timelapse cases as shown in the bottom row of Figure 1. The peak timelapse anomaly is observed at 7km offset and 0.1Hz frequency. These acquisition parameters are then used to produce 2D maps of CSEM responses for the entire simulation cells for the timelapse intervals 2004 – 1998 (six years), 2006 – 1998 (eight years) and 2008 – 1998 (ten years). Figure 2 shows the CSEM modelling results.

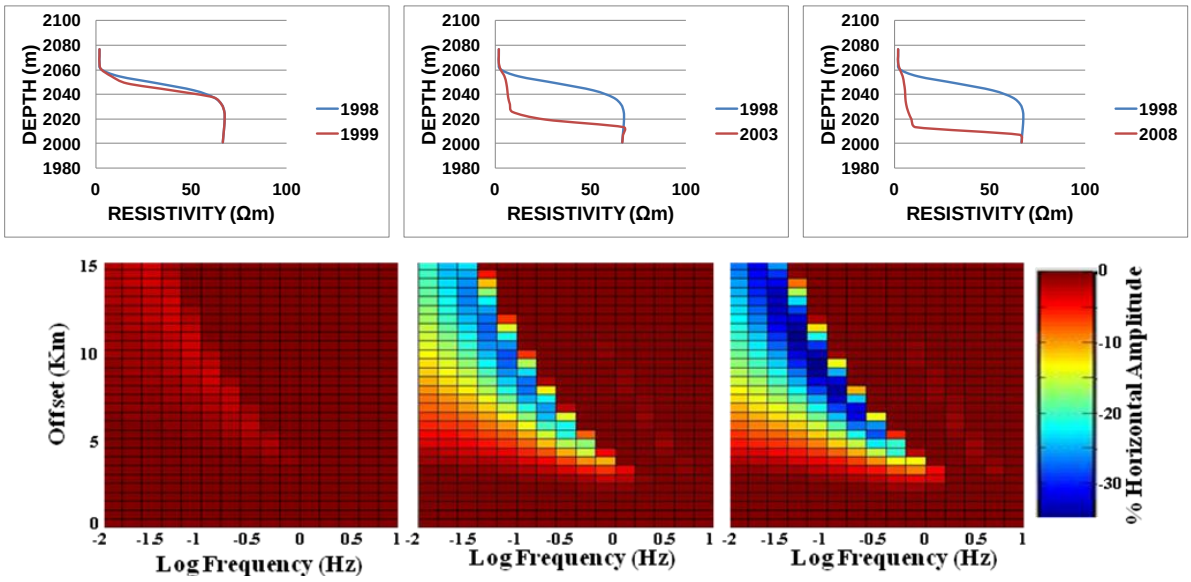

Figure 1 *Top row shows the graphs of depth versus resistivity as a function of time. The blue curve represents the baseline resistivity while the red curve is the monitor resistivity which changes with time (one, five and ten years) from left to right. Bottom images show the corresponding percentage CSEM horizontal amplitudes with respect to the survey offset and the frequency.*

Results and Discussion

Figure 2 shows that the timelapse CSEM maps correctly indicate areas of the reservoir in which the water saturation is changing, as production and injection activities progress. It particularly shows the water flooding front, which is helpful in terms of providing early warning of water encroachment onto production well. The results also indicate zero timelapse CSEM signals for the part of the reservoir where there are no changes in the reservoir model. Although this CSEM signal clearly suggests that the reservoir is not changing, it does not in itself indicate whether that portion of the reservoir is water or hydrocarbon charged unless the initial conditions of the reservoir are known. Calibration to well activities is therefore very important and we observe here that the repeated CSEM signatures are more pronounced near the injector rather the producer wells. For each of the CSEM surveys (not shown here), the measured signal ranges between 7.2×10^{-14} and $12.1\times10^{-14} V/Am^2$, which is above the noise floor we expect to see for this water depth (somewhere between 10^{-14} and $10^{-15} V/Am^2$). The signal difference is at most about $-4\times10^{-14} V/Am^2$, which constitutes a timelapse CSEM magnitude of about -32% amplitude change and 32° phase difference, which are above the 5% and 5° possible timelapse noise floor. Although 1D responses are calculated, we would expect this to be a best case scenario. When higher dimensional effects are taken into account it is likely that the changes will be smaller. However qualitatively, it can be observed that changes in the water saturation can be mapped by taking the timelapse electromagnetic measurements at different calendar times.

Figure 3 shows that timelapse CSEM is a combination of the spatially varying reservoir parameters and the dynamically varying water saturation, rather than just the dynamic change in water saturation. Thus, initial knowledge of the distribution of these variables is important in constraining the direct measurement of change in water saturation from the timelapse CSEM. Having established a good correlation between the timelapse CSEM responses and the changing reservoir variables, we then carried out 4D seismic modelling. The sensitivities of the timelapse CSEM and the 4D seismic to the change in water saturation are compared using the cross-plots shown in Figure 4. It can be concluded from Figure 4 that the CSEM is more sensitive and consistently more linearly related to the change in water saturation than the seismic. This is not surprising because seismic is sensitive to both saturation and pressure changes, and these parameters cannot be easily separated on the basis of seismic alone.

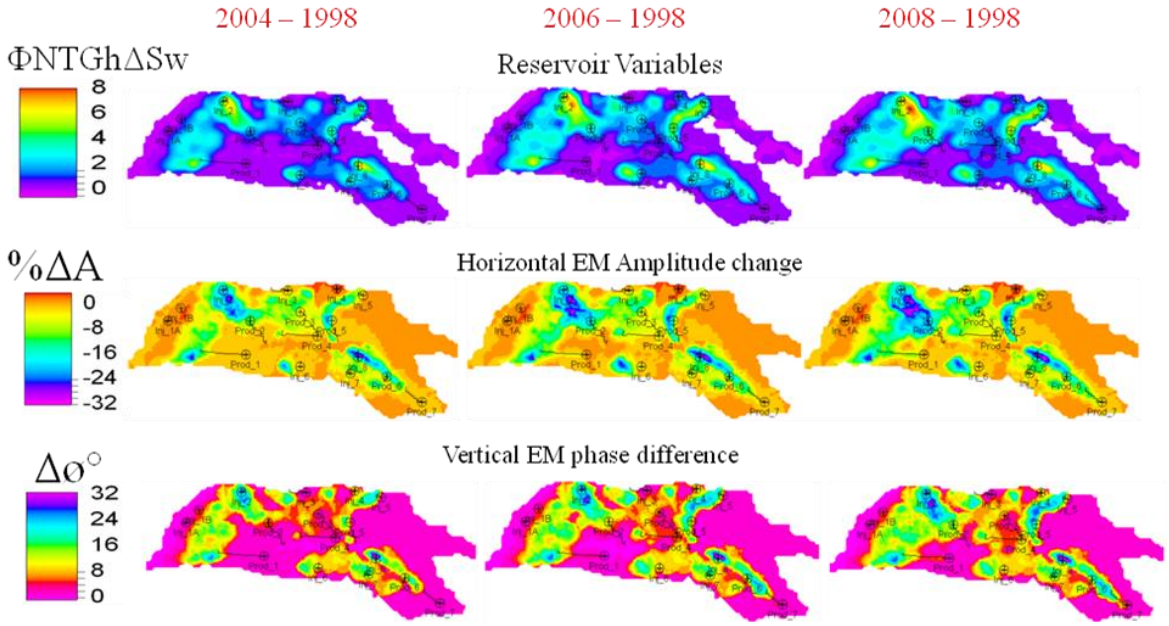

Figure 2 *Top row images show the different timelapse maps of the reservoir variables induced by changes in water saturation between the various monitor models and the baseline model (years in red). The middle and the bottom rows are the corresponding timelapse CSEM responses, the percentage horizontal amplitude and the vertical phase difference respectively.*

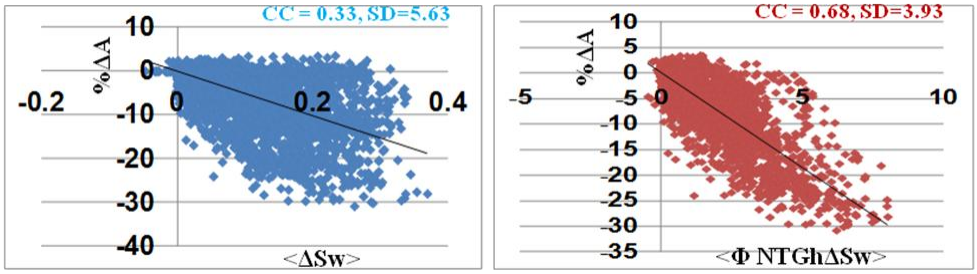

Figure 3 *The cross-plots of timelapse CSEM amplitude against the depth averaged reservoir variables (2008 - 1998). On the left (only change in water saturation), on the right (combination of spatial variation of net-to-gross, porosity, thickness and change in water saturation). CC (correlation coefficient), SD (standard deviation)*

In line with the seismic equation given by Falahat et al. (2011) to relate 4D seismic to the reservoir variables, we propose that time-lapse EM amplitude (ΔA) and phase differences $(\Delta\phi)$ vary with dynamic and spatial change in water saturation (ΔS_w), spatially varying effective porosity $(\Phi NTG)_w$ and reservoir thickness (h_w) according to:

$$\Delta A = c(\Phi NTG)_w h_w \Delta S_w \,, \tag{2}$$

and

$$\Delta\phi = d(\Phi NTG)_w h_w \Delta S_w \,, \tag{3}$$

If frequent CSEM surveys with permanent seabed sensors are possible, then a continuous monitoring of reservoir fluid production and injection activities would be achievable. This will depend upon the cost benefit and the time gap between acquisition, processing and data interpretation. Processing in this case will include repeatability and anomaly registration issues.

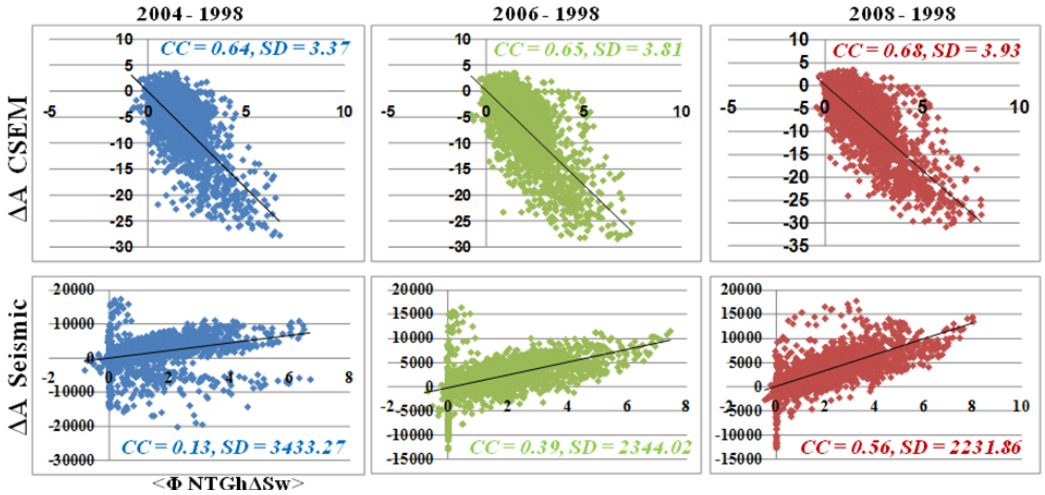

Figure 4 *Top and bottom rows show the graphs of timelapse CSEM and 4D seismic amplitudes cross-plotted against the reservoir depth averaged variables (combination of spatial variation of net-to-gross, porosity, thickness and change in water saturation) respectively.*

Conclusions

We have shown that timelapse EM responses (in this case horizontal amplitude and vertical phase) are sufficiently linear with change in saturation (ΔSw) despite reservoir heterogeneity, that ΔSw could directly be interpreted and estimated from the timelapse EM measurements. However, such saturation measurements still need to be constrained with the knowledge of the spatial distribution of porosity, net-to-gross and reservoir thickness.

Acknowledgements

We thank sponsors of the Edinburgh Time Lapse Project, Phase IV (BG, BP, Chevron, ConocoPhillips, ENI, ExxonMobil, Hess, Ikon Science, Landmark, Maersk, Marathon, Norsar, Petrobras, RSI, Shell, Statoil and Total) for supporting this research. We thank Schlumberger-Geoquest for the use of their Petrel and Eclipse software. Olarinre Salako is on leave of absence from the Department of Geology, Osun State University, Nigeria. He acknowledges the financial support from the Petroleum Technology Development Fund, Nigeria.

References

Archie, G.E. [1942] The electrical resistivity log as an aid in determining some reservoir characteristics. *Petroleum Transactions of the AIME*, **146**, 54–62.

Falahat, R., Shams, A. and MacBeth, C. [2011] Adaptive engineering-based scaling for enhanced dynamic interpretation of 4D Seismic.*73rd EAGE Conference, Expanded Abstracts, Vienna, Austria*.

Key K. [2009] 1D inversion of multicomponent, multifrequency marine CSEM data: Methodology and synthetic studies for resolving thin resistive layers. *Geophysics*, **74**(2), F9-F20.

Landrø M. [2001] Discrimination between pressure and fluid saturation changes from time-lapse seismic data. *Geophysics*, **66**(3), 836–844.

Liang, L., Abubakar, A. and Habashy, T.M. [2011] Feasibility study of marine CSEM for reservoir monitoring using joint 3D EM modeling and fluid flow simulator. *73rd EAGE Conference, Expanded Abstracts, Vienna, Austria*.

Lien, M. and Mannseth, T. [2008] Sensitivity study of marine CSEM data for reservoir production monitoring. *Geophysics*, **73**(4), F151–F163.

MacBeth, C., Floricich, M. and Soldo, J. [2006] Going quantitative with 4D seismic analysis. *Geophysical Prospecting*, **54**, 303 – 317.

Orange, A., Key, K. and Constable, S. [2009] The feasibility of reservoir monitoring using time-lapse marine CSEM. *Geophysics*, **74**(2), F21–F29.

Shahin, A., Key, K., Stoffa, P.L. and Tatham, R.H. [2010] Time-lapse CSEM analysis of shaly sandstone simulated by comprehensive petro-electric modeling. *80th Annual Meeting, SEG, Expanded Abstracts*, 889–894.